

Atmospheric dispersion correction for the Subaru AO system

Sebastian Egner^a, Yuji Ikeda^b, Makoto Watanabe^c, Y. Hayano^a, T. Golota^a,
M. Hattori^a, M. Ito^a, Y. Minowa^a, S. Oya^a, Y. Saito^a, H. Takami^a, M. Iye^d

^aNational Astronomical Observatory of Japan, 650 N. A'ohoku Place, Hilo, HI, 96720, U.S.A.;

^bPhotocoding, Hashimoto, Japan;

^cHokkaido University, Sapporo, Japan;

^dNational Astronomical Observatory of Japan, Mitaka, Japan;

ABSTRACT

In this paper, we present the science path ADC unit (atmospheric dispersion corrector) for the AO188 Adaptive Optics System of the Subaru Telescope. The AO188 instrument is a curvature-based Adaptive Optics system with 188 subapertures and achieves good correction down to shorter wavelengths like J-band. At these wavelengths, the atmospheric dispersion within the band becomes significant and thus a correction of the atmospheric dispersion is essential to reach diffraction-limited image quality. We give an overview of the requirements, the final optical and mechanical design of the ADC unit, as well as the structure of its control software.

Keywords: Adaptive Optics, Atmospheric dispersion, ADC, high angular imaging

1. INTRODUCTION

The second generation adaptive optics system at the Subaru telescope was recently commissioned. The AO188^{1,2} system is based on the curvature sensor principle and uses 188 elements for wavefront measurement and correction. It has both a natural guide-star (NGS) mode, as well as a sodium laser guide-star (LGS) mode.

AO188 can be used with two primary science instruments. IRCS³ (infrared camera and spectrograph) is an infrared imager with z, J, H, K', K, L and M-band imaging with 12, 20 and 52 mas/pixel. It can also perform spectroscopy with a spectral resolution of up to 20 000. The second main science instrument for AO188 is HiCIAO⁴ (High Contrast Instrument for the Subaru Next Generation Adaptive Optics). HiCIAO is a coronagraphic imager with three observing modes: direct imaging, polarization differential imaging, and spectral differential imaging.

However, especially at larger zenith angles and at shorter wavelengths, the differential atmospheric refraction, or dispersion, becomes important. Atmospheric dispersion is caused by the dependence of the index of refraction on the wavelength of the light. Light rays with shorter wavelength are refracted more than rays with longer wavelength. For a star, which is not at the zenith, this means that the apparent location of the star depends on the wavelength. This of course implies that for a certain filter bandwidth the star will look elongated, with the red end closer to the horizon and blue end closer to zenith.

Figure 1 shows the atmospheric dispersion as a function of the wavelength and for different zenith distances. For example for a filter bandwidth from 1.0 to 1.5 micron, a star at 60 deg zenith distance will be elongated by 0.19 arcsec. This is approximately 5 times as large as the radius of the Airy disk at this wavelength for an 8m telescope, which is 0.038 arcsec.

The impact of atmospheric dispersion is even worse for coronagraphic imaging. For an elongated PSF, a significant portion of the light can pass the occulting mask and leak into the science image, thus destroying the achievable contrast. For observations with Adaptive Optics at the diffraction limit, a good correction of the atmospheric dispersion is thus mandatory to tap the full potential of this technique. This is true both for angular resolution, as well as for coronagraphic contrast.

Send correspondence to S. Egner, E-mail: egner@naoj.org, phone: +1 808 934 5949

2. OPTICAL DESIGN

2.1. Requirements

The basic optical design⁵ of the ADC of AO188 consists of two identical prisms, which are mounted close to the pupil plane in the collimated light (see fig. 2). Both prisms can be rotated around the optical axis to adjust the amount of atmospheric dispersion correction.⁶ For a rotation angle of 0 deg of the second prism with respect to the first prism, the dispersion of the first prism is canceled by the second prism. For any other rotation angle, the dispersion of the first prism is only partially canceled by the second prism. For the compensation of the atmospheric dispersion, the rotation angle of the two prisms is therefore adjusted according to the zenith distance of the observed object.

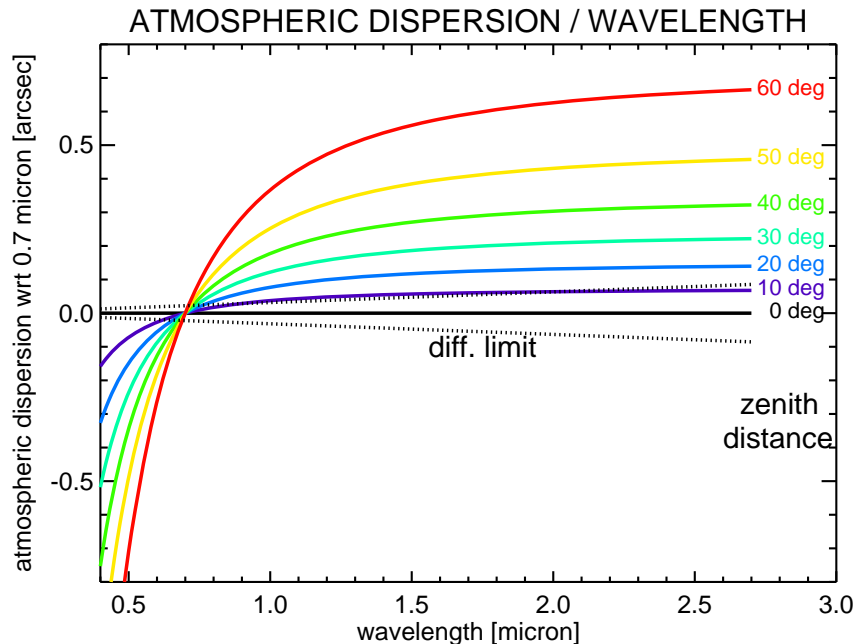
The goal of the optical design of the science path ADC was to achieve a good correction for all relevant wavelengths, starting from the visible for wavefront sensing, to the infrared for science imaging.

The high-level optical specifications of the ADC prisms are:

1. residual spot elongation after correction (imaging/spectroscopy): $< 10\%$ of diffraction-limited PSF
2. residual spot elongation after correction (chronography): $< 1/30$ th of diffraction-limited PSF diameter
3. spot motion during rotation: < 2 arcsec
4. working zenith distances: 0 to 63 deg
5. wavelength range: 0.45 to 2.2 micron

2.2. Optical Design

The optical design to meet these specifications is based on two double prisms, as shown in figure 2. To evaluate the capability of this configuration for dispersion correction, we determined the atmospheric dispersion with and without correction by the ADC as a function of the wavelength for each science filter. As shown in figure 3, atmospheric dispersion at 60 deg zenith distance can elongate the PSF by a factor of 1.6. After correction with



graphic file plot_dar_zemax.ps created by: plot_dar_zemax.pro on Fri Apr 30 22:28:55 2010

Figure 1. The atmospheric dispersion as a function of the wavelength. The various curves correspond to different zenith distances.

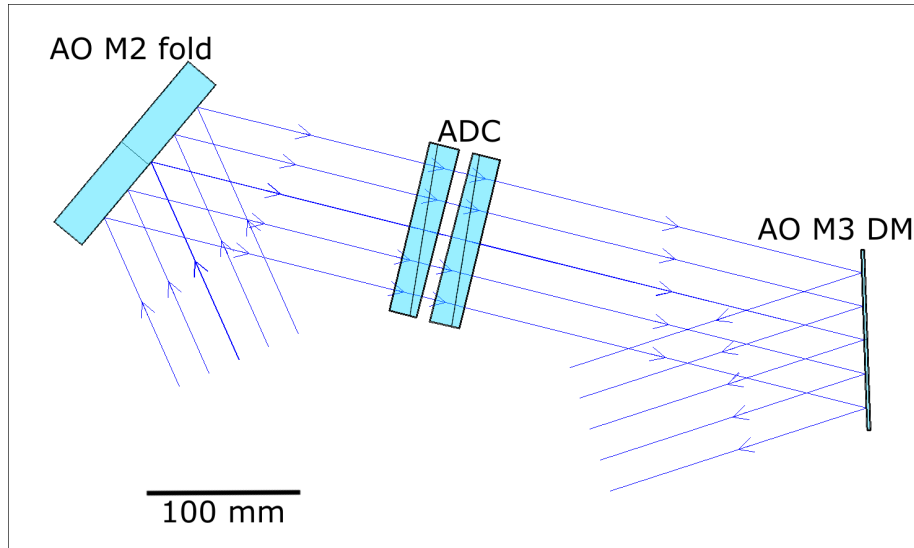


Figure 2. A zoom of the optical components in the area around the ADC unit in AO188. The two prisms of the ADC unit are located in front of the deformable mirror (DM) in the collimated beam. In this picture the second prism is actually reversed and rotated by 180 deg around the optical axis with respect to the first prism.

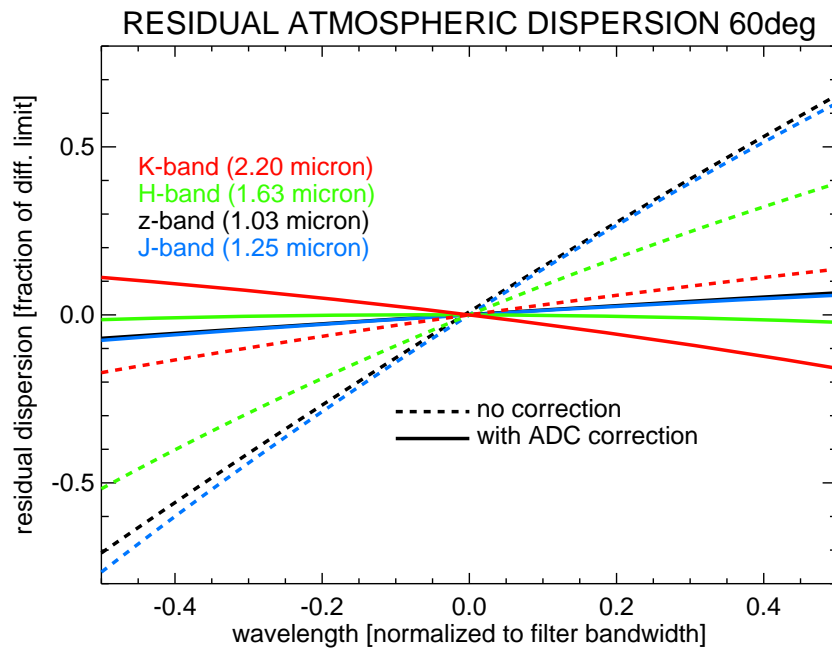


Figure 3. The atmospheric dispersion as a function of the normalized wavelength within each filter of IRCS for a zenith distance of 60 deg. Without the correction by the ADC (dashed lines), the atmospheric dispersion can reach up to 60% of the diffraction limited PSF. This means that the PSF will be elongated by a factor of 1.6 along the elevation axis. With the correction by the ADC (solid lines), the linear term of the dispersion is gone and a small quadratic residual dispersion remains. The rotation angle of the ADC prisms are adjusted to achieve the optimal correction for all filters simultaneously. Therefore the dispersion in K-band has still a small residual linear component.

the ADC unit, the residual dispersion is less than 15% of the diffraction limit. This figure shows that the ADC can correct the linear term of the atmospheric dispersion. Only a quadratic residual remains.

To make this more illustrative, figure 4 shows the internal PSF of AO188 with and without the ADC correction. The elongation of the PSF due to the atmospheric dispersion can be clearly seen. The small coma aberration in the corrected PSF is due to the dichroic mirror of AO188, which is a tilted wedge in the converging beam.

2.3. Rotation angle

The optimal rotation angle $\alpha(z)$ of the ADC prisms as a function of the zenith distance was determined for all science filters. For IRCS we found that the same $\alpha(z)$ can be used for all filters. The correction of the dispersion will not be optimal, but within the requirements defined above. Figure 5 shows the optimal rotation angle for the various filters of IRCS as a function of the zenith distance.

However, for HiCIAO, the requirements are much tighter. The requirement to achieve the desired contrast for HiCIAO is that the PSF is spread by no more than 1/30th of the PSF size for all the wavelengths within a certain science filter. This can only be achieved by using a dedicated $\alpha(z)$ function for each filter of HiCIAO.

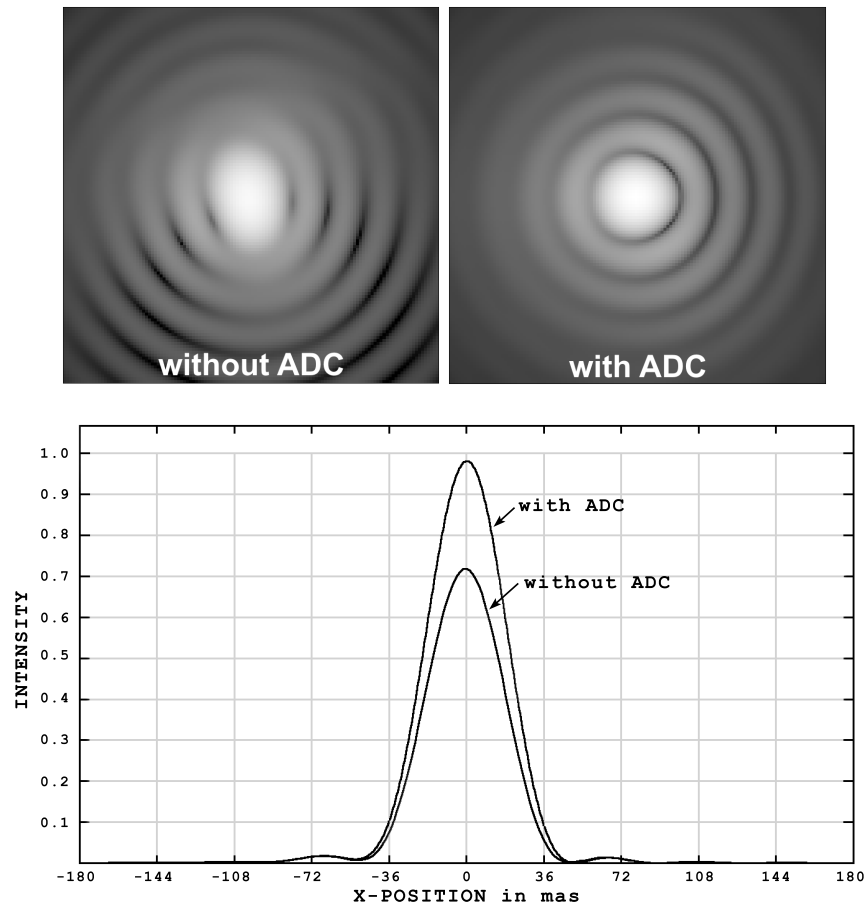


Figure 4. The PSF in H-band with and without the correction of the atmospheric dispersion by the ADC unit. This is the internal PSF of the AO system only, no central obstruction or spiders of the telescope have been taken into account. The field-of-view is 2.3×2.3 arcsec. Without the ADC unit, the internal Strehl-ratio drops to 72% and is restored to 98% with the ADC unit.

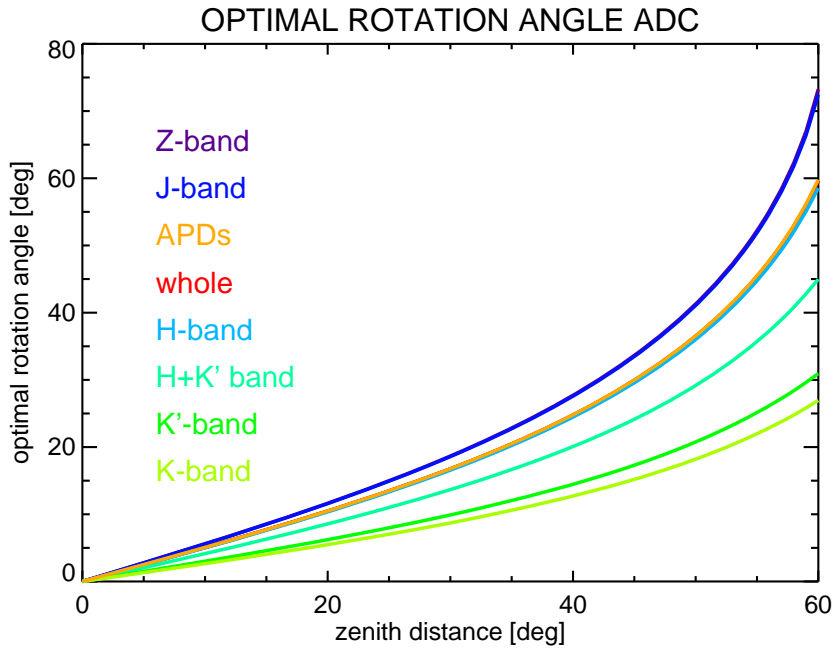


Figure 5. The optimal rotation angle of the two prisms with respect to each other for the various science filters used, as a function of the zenith distance. "Whole" means that the rotation angle was optimized for all filters simultaneously.

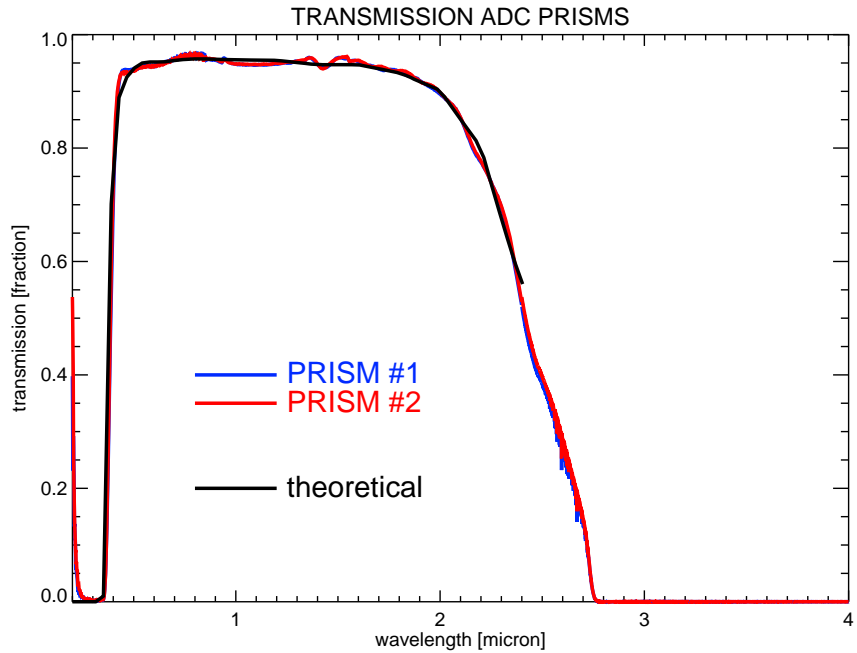


Figure 6. The transmission of the ADC unit as a function of the wavelength. The measured transmission for both prisms match very well the theoretically expected transmission based on the used glass types.

Figure 5 verifies that the rotation angle α_{ad} of the prisms to correct for the atmospheric dispersion can be described as:

$$\cos \alpha_{\text{ad}} = c_f \cdot \tan z , \quad (1)$$

with the zenith distance z , and the calibration factor c_f , which depends on the used science filter.

2.4. Transmission

Having glasses in the optical path has an impact on the throughput of the instrument. To analyze this impact, we measured the transmission of the manufactured prisms with a spectrograph. As shown in figure 6, the measured transmission follows very nicely the theoretically expected transmission. This also highlights that the anti-reflection coating is efficiently suppressing reflection. In the relevant wavelength range from 0.45 to 2.0 micron the transmission is higher than 90 %.

3. MECHANICAL DESIGN

3.1. Requirements

To support the prisms and to precisely rotate them for following the elevation of the telescope, a mechanical structure had to be newly designed. Additionally, because of possible wavefront aberrations introduced by the prisms, the low throughput of the prisms and since a dispersion correction is not necessary for the longer wavelengths like K to M band, the ADC unit has to be able to be retracted from the optical beam.

In summary, the main critical specifications of the mechanical structure are:

1. insert / retract the unit within 20 seconds
2. repeatability of rotation: better than 0.087 deg
3. step size of rotation: less than 0.087 deg
4. backlash of rotation: less than 0.2 deg
5. maximal rotation velocity: more than 3.75 deg/sec
6. separation tolerance on prisms: better than 0.5 mm
7. tilt of prisms: less than 1.0 deg
8. tilt of entire unit: less than 1.0 deg
9. clear aperture: more than 120 mm

3.2. Mechanical Design

As already shown in figure 2, the clearance around the ADC unit is very small. Including an insert and retract mechanism of the ADC unit while avoiding vignetting of the beam thus turned out to be challenging. Furthermore, the accuracy for the rotational unit has to be high and the backlash very small by using 2-phase stepper motors, which can be controlled from the current controller system developed for the other automation units of AO188.

These requirements were accomplished by the combination of hyperthin-cross-roller bearings and a newly developed ball-reducer. The radial and axial thicknesses of the bearing are only 8 mm, even for a diameter of 156 mm. And, the backlash of the ball-reducer is less than a few arcmin by not employing toothed gears, but many steel balls for reduction. For the sensor of the homing position we used hall elements, which emit no light and enable the high position accuracy of less than $30 \mu\text{m}$. The mechanical design and manufacturing according to the specifications was done by Photocoding in Japan. A drawing of the mechanical design can be seen in figure 7. An overview of the AO188 instrument with the ADC installed is shown in figure 8.

4. SOFTWARE DESIGN

4.1. Requirements

For the control of the prisms' rotation angles, as well as for inserting and retracting the ADC unit, a dedicated software was developed. This software is part of the science path control software. It acts as a server and does not initiate any interactions with other components of the telescope or instrument control software. This is essential for development and debugging. A change in the pointing of the telescope or science filter is initiated by a higher-level control software and sent to the science path server software. The same concept is also implemented for the other sub-systems of AO188. The coordination of all the subsystems in AO188 is accomplished in the higher-level software.

The high-level specifications for the tracking accuracy of the ADC prisms are the following:

1. minimal zenith distance: less than 1 deg
2. step size: less than 0.087 deg
3. update frequency: less than 0.58 sec
4. tracking modes: sidereal, non-sidereal, pupil

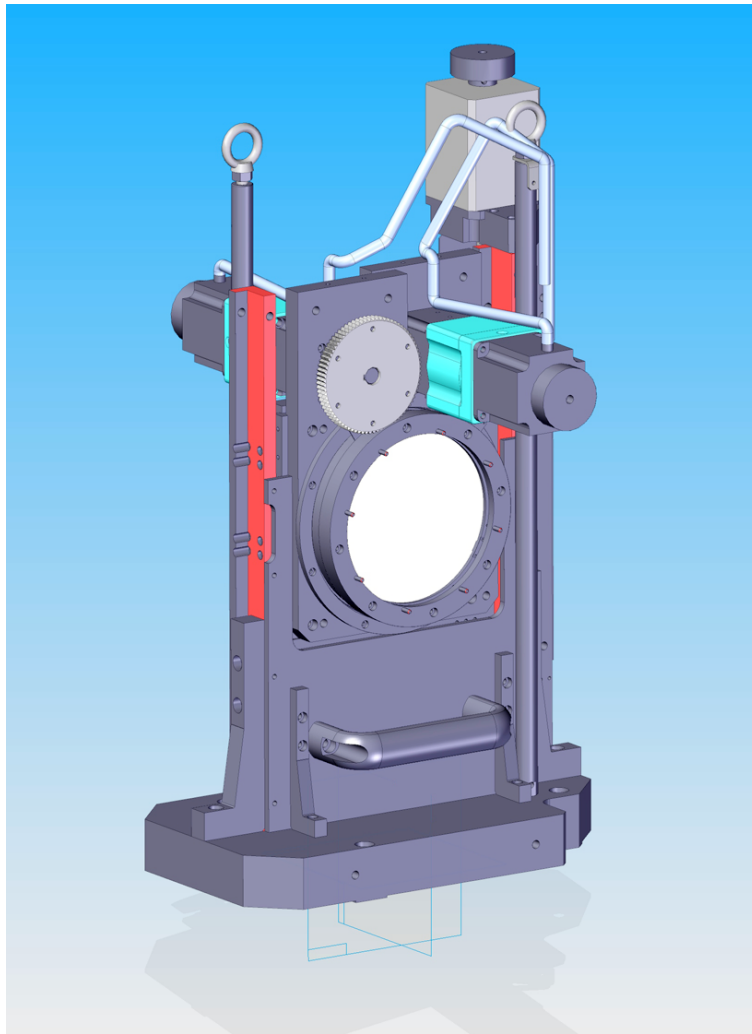


Figure 7. A CAD drawing of the opto-mechanical design of the ADC unit.

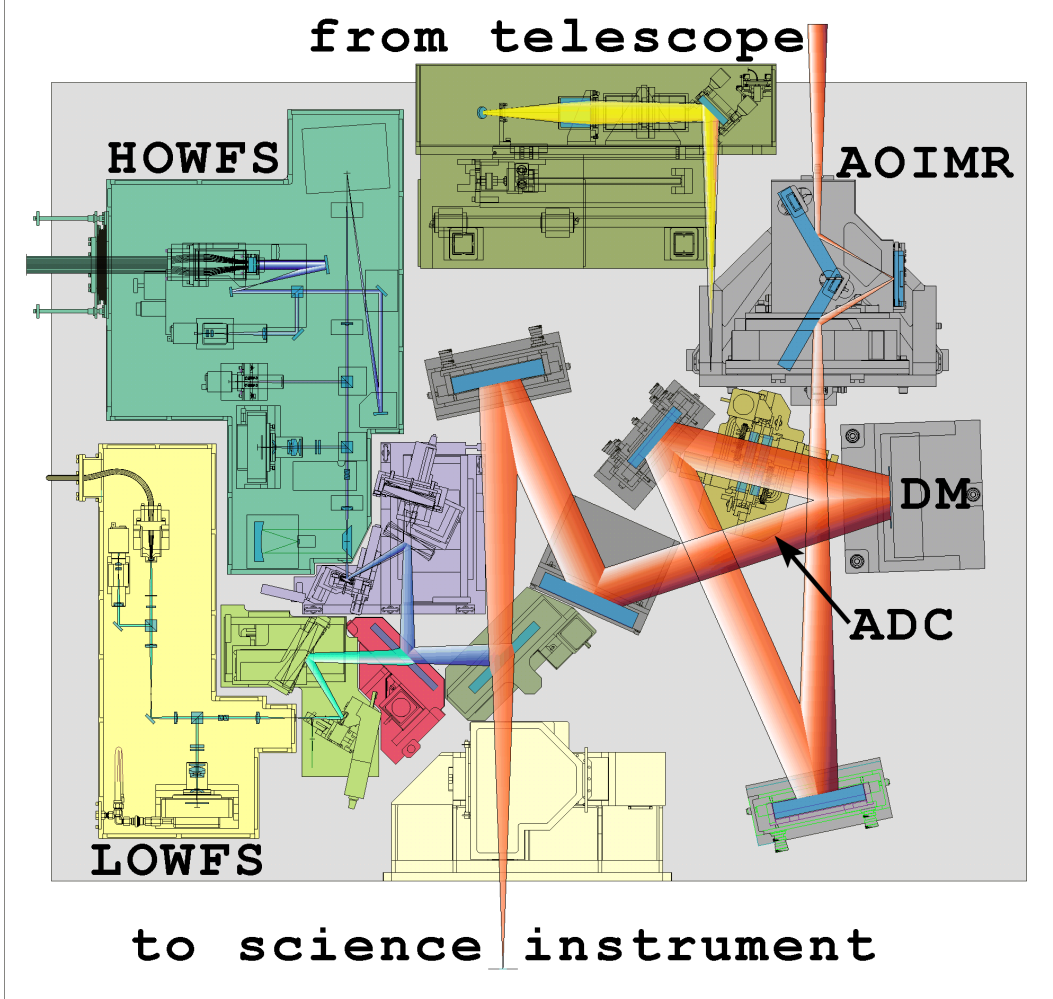


Figure 8. The opto-mechanical layout of the AO188 instrument. The ADC unit is located in the collimated beam in front of the Deformable Mirror. For more details about the AO188 components, see Hayano et al.¹

4.2. Tracking function

As mentioned above and shown in figure 8, the ADC unit is located behind the image rotator. This means that the direction of the elevation axis at the ADC unit is constantly changing because of the parallactic angle tracking of the image rotator. Therefore the rotation angles of the two prisms are given by a combination of those two rotations.

The rotation angle α_{ad} of the prisms to correct for the atmospheric dispersion was determined in equation 1. The second component, which is the rotation angle α_{pa} of the elevation axis in sidereal tracking after the image rotator, is given by:

$$\tan(\alpha_{pa}) = \frac{\sin h}{\tan \phi \cos \delta - \sin \delta \cos h} , \quad (2)$$

with the zenith distance z , the hour angle h , the declination δ of the object and the latitude ϕ of the telescope.

The total rotation angle α_p of the two prisms is thus:

$$\alpha_p = \alpha_{pa} \pm \alpha_{ad} . \quad (3)$$

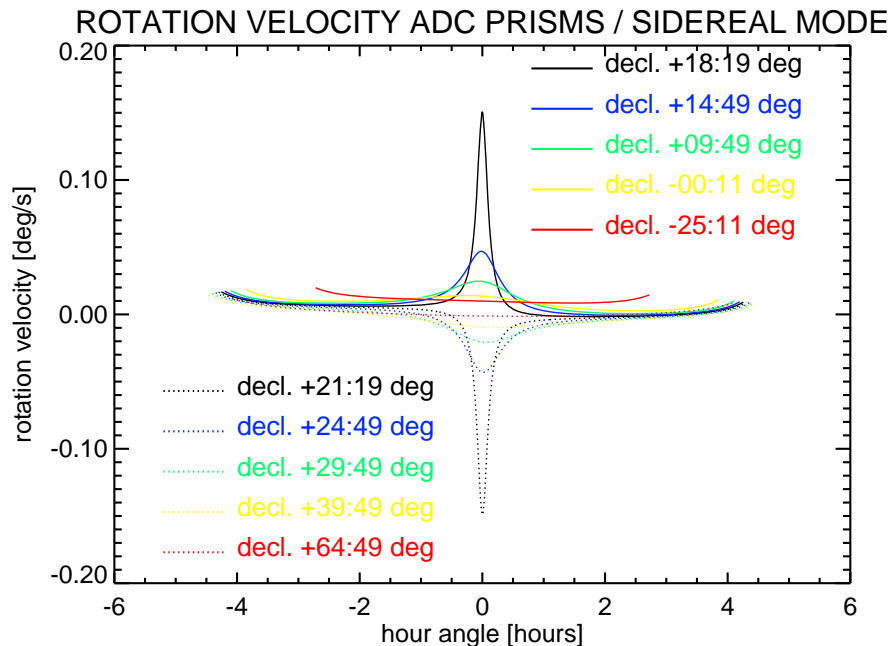


Figure 9. The rotation velocity of the ADC prisms as a function of the hour angle of the object. The different colors correspond to different values of the declination of the objects.

As shown in figure 9, the rotation velocity of the ADC prisms in sidereal mode is at the maximum 0.15 deg/s. Comparing this to the step size, the timing accuracy for tracking is thus given to be of the order of half a second. For the implementation of the tracking of the prisms it is thus sufficient to calculate the rotation angle α_p and update the positions of the prisms with a frequency of 2 Hz. This can be done by the instrument control computer.

5. CONCLUSION

In this paper we presented the ADC unit for the science path of the second-generation Adaptive Optics system for the Subaru telescope (AO188). We defined the high-level requirements of this unit, and showed in detail how those can be converted to requirements for the optics and mechanics. Finally we presented the actual opto-mechanical design and implementation of this unit. The on-sky performance verification will be done later this year.

REFERENCES

1. Y. Hayano, H. Takami, *et al.*, “Commissioning status of Subaru laser guide star adaptive optics system,” in *SPIE*, 7736, 2010.
2. Y. Minowa, Y. Hayano, *et al.*, “Performance of Subaru adaptive optics system AO188,” in *SPIE*, 7736, 2010.
3. H. Terada, N. Kobayashi, A. Tokunaga, *et al.*, “Performance update of the infrared camera and spectrograph for the Subaru Telescope (IRCS),” in *SPIE*, 5492, 2004.
4. K. W. Hodapp, R. Suzuki, M. Tamura, *et al.*, “HiCIAO: the Subaru Telescope’s new high-contrast coronagraphic imager for adaptive optics,” in *SPIE*, 7014, 2008.
5. M. Watanabe, H. Takami, N. Takato, *et al.*, “Design of the Subaru laser guide star adaptive optics module,” in *SPIE*, 5490, 2004.
6. E. Wallner and W. Wetherell, “Atmospheric Dispersion Correctors with Broad Spectral Bandpass for Large Telescopes,” in *Optical and Infrared Telescopes for the 1990’s*, 1980.